JACS
JOURNAL OF THE AMERICAN CHEMICAL SOCIETY

Perspective

pubs.acs.org/JACS

Defect Chemistry for Thermoelectric Materials

Zhou Li, Chong Xiao,* Hao Zhu, and Yi Xie*

Hefei National Laboratory for Physical Sciences at the Microscale, Collaborative Innovation Center of Chemistry for Energy Materials, University of Science & Technology of China, Hefei, Anhui 230026, P. R. China

ABSTRACT: Defect engineering, at the core of the field of thermoelectric studies, serves as a scaffold for engineering the intrinsic electrons' and phonons' behaviors to tailor thermoelectric parameters through the direct impacts of band engineering and phonon engineering, which can modify electronic band structure and phonon transport behavior to enhance the power factor (PF = σS^2) and reduce the lattice thermal conductivity (κ_l). By virtue of the implementation of defect engineering, the past decades have witnessed great progress in thermoelectric research through synergistic optimization of the inter-correlated transport parameters, and substantial enhancement has been achieved in the performance of various thermoelectric materials. However, current established optimization strategies based on defect engineering are mainly focused on tuning the electronic and phonon structures, while modulation by additional degrees of freedom caused by defects has long been neglected. In this Perspective, we focus on our interest in the under-exploited aspects of defect engineering, which include defect-related spin effects, defect-mediated atom or charge migration effects, and defect-related interface effects. Through these new points of view, we hope to arouse intense attention to the overlooked parts of defect engineering and combine them with current optimization strategies from the perspective of multiple degrees of freedom modulation, to enable the full potential of defect engineering for boosting thermoelectric performance. Finally, based on the discussion herein and current achievements in thermoelectric research, some personal perspectives on the future of this field are also presented.

INTRODUCTION

The dwindling availability of fossil fuels and concerns about greenhouse gas emissions[1] highlight the ever-growing demand for alternative "green" renewable energy, as well as the establishment of new energy conversion technologies with increased efficiency.[2−5] Within this context, thermoelectric technology, which is able to achieve reversible conversion between electricity and heat on the basis of the propagation of electrons and phonons, has been recognized as a potential candidate to alleviate the energy and environment crisis by recycling waste heat and has been extensively studied worldwide.[6−9] However, an inconvenient truth is that, although much time and effort has been invested in research and development into this energy conversion technology since its discovery, large-scale commercialization of thermoelectric technology is still in its infancy, mainly attributed to the low energy efficiency,[6,10−12]

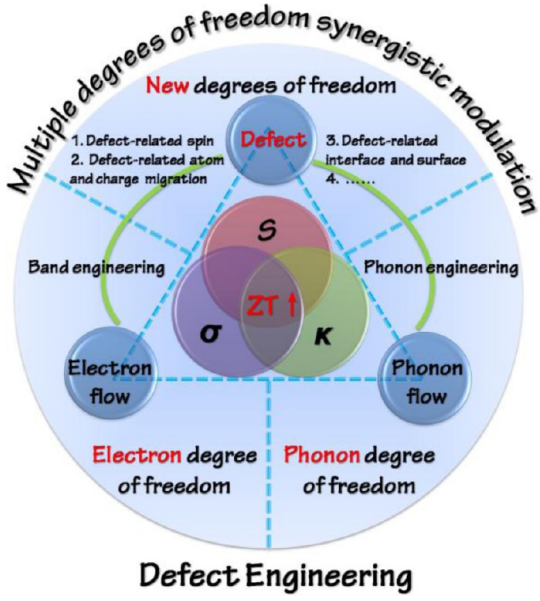

Figure 1. Schematic illustration of the ZT optimization strategies based on defect engineering from the perspective of multiple degrees of freedom synergistic modulation.

which is gauged by a dimensionless figure of merit quantified as $ZT = \sigma S^2 T/(\kappa_e + \kappa_l)$, where σ is the electrical conductivity, S is the Seebeck coefficient, T is absolute temperature, and κ_e and κ_l are the electronic and lattice components of the total thermal conductivity.[13,14] The non-trivial roadblock lies in the strong interdependence between electrical and thermal parameters.[11,12,15]

It is worth noting that, in a thermoelectric solid, the parameters governing the ZT performance are essentially the external manifestations of the electron (hole) flow, phonon flow, and their intercoupling, mediated by defects.[16] This leads to the use of defect engineering[17−19] to optimize thermoelectric properties via intentional manipulation of the type, size, concentration, and spatial distribution of defects, which can serve as a scaffold for engineering the intrinsic electrons' and phonons' behaviors to tailor the thermoelectric parameters.[16,20−24] Given the lower inter-dependence between the electrical properties and the lattice thermal conductivity, defect engineering can impact the thermoelectric property via two basic strategies: band engineering, which can enhance the power factor (PF = σS^2) by tuning the electronic band structure, and phonon engineering, which can reduce κ_l by enhancing phonon scattering (as illustrated in Figure 1).[20−22,25] In fact, the past decades have witnessed significant

Received: August 21, 2016
Published: October 19, 2016

DOI: 10.1021/jacs.6b08748
J. Am. Chem. Soc. 2016, 138, 14810−14819

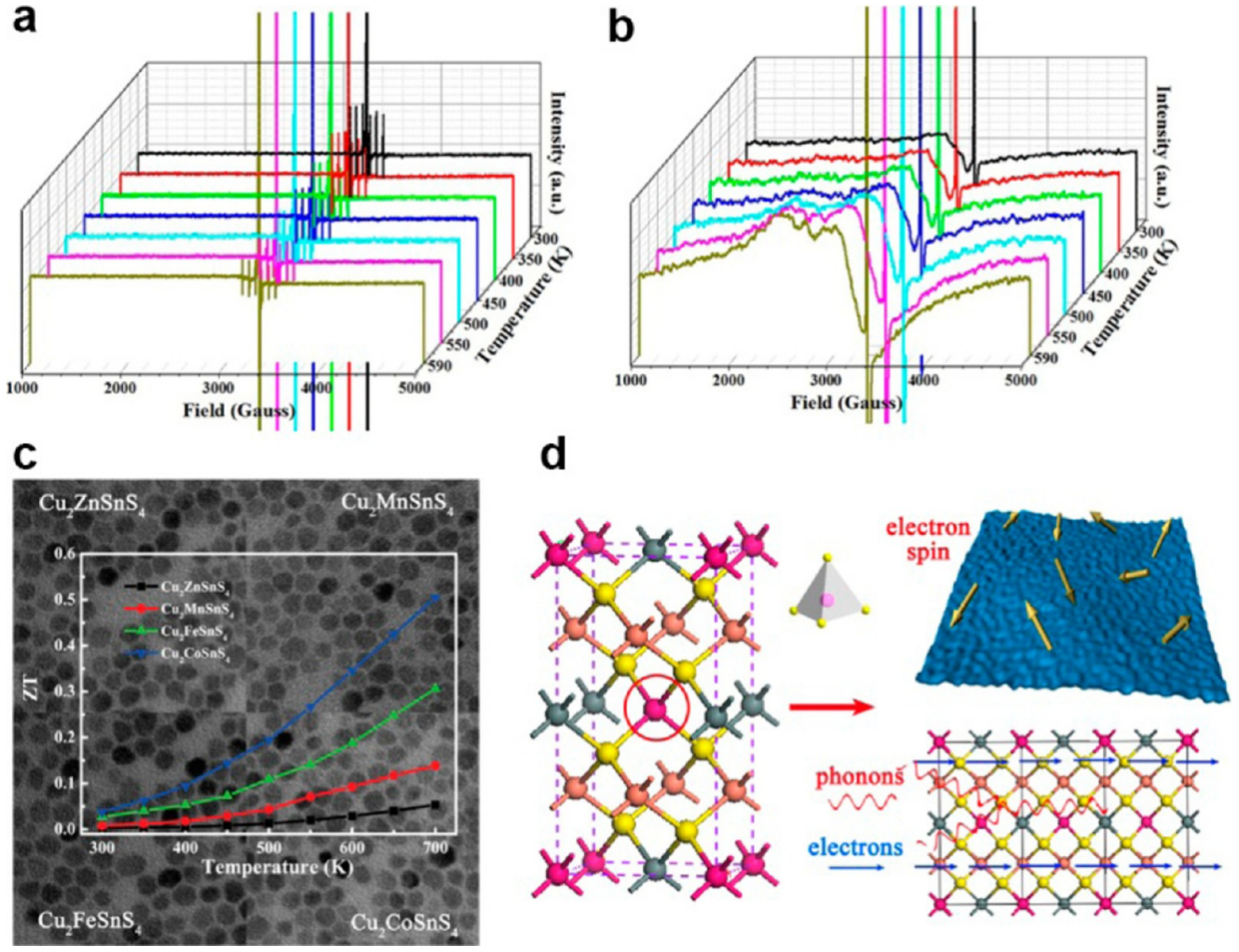

Figure 2. (a,b) Comparison of the temperature-dependent electron paramagnetic resonance signals for pristine (a) and Ni-doped (b) Cu_2ZnSnS_4 nanocrystals. (c) Comparison of the ZT values for Cu_2XSnS_4 (X = Zn, Mn, Fe, Co) nanocrystal composites. The background shows their TEM images. (d) Schematic illustration of the different scattering mechanisms in Cu_2XSnS_4 nanocrystal-based composites, including electron spin and electron and phonon scattering. Adapted with permission from ref 39. Copyright 2014 The Royal Society of Chemistry.

progress in thermoelectric technology through the implementation of defect engineering, and substantial enhancement of the ZT performance has been achieved in various thermoelectric materials.[7,8,21,26−37] However, for defect engineering, this is only half of the story. Current established optimization strategies based on defect engineering are mainly focused on tuning of the electronic and phonon structures, which is far less than what defects can do. Actually, additional modulation degrees of freedom via defect engineering including defect-related spin tunning,[38−42] vacancy-mediated atom or charge transfer,[43,44] surface distortion,[46] and so on have begun to show up in thermoelectric studies. We believe that, once combined with the existing electronic and phonon structure optimization strategies, these new enhancements can enable the utmost efficiency of defect engineering.

Therefore, in this Perspective, we focus our interests on the under-exploited aspects of defect engineering, including defect-related spin effects (spin entropy, Kondo effect, and spin-state transition), defect-mediated atom or charge migration effects (atom exchange and interlayer charge transfer), and defect-related interface effects (homojunctions and surface distortion). By presenting these different points of view in this Perspective, we hope to arouse attention to the overlooked aspects of defect engineering, such that they might be combined with the established strategies of tuning electronic and phonon structures from the perspective of multiple degrees of freedom synergistic modulation, to enable the full potential of defect engineering for boosting thermoelectric performance (as illustrated in Figure 1). We believe that the concept of synergistic modulation via multiple degrees of freedom is superior and critical for the further development of thermoelectric technology, and we expect that presenting this idea will stimulate a new round of prosperity in thermoelectric studies. Finally, on the basis of the discussion presented herein and current achievements in thermoelectric research, we give some personal perspectives on potential research directions for this field.

■ DEFECT-RELATED SPIN EFFECT

As an intrinsic property of electrons, spin can be engineered by introducing crystal defects and used to tailor the related thermoelectric parameters. For example, the entropy carried by electron spin (also called spin entropy) increases when a crystal is doped with magnetic ions with unpaired 3d or 4f electrons, which is favorable for enhancement of the Seebeck coefficient.[39,40] In fact, these localized magnetic moments can interact with the electron spin (Kondo interaction/effect), resulting a giant Seebeck coefficient.[40] In addition, rich spin configurations, which are widespread in transition-metal oxides ($Ca_3Co_4O_9$ etc.), can be modified by aliovalent doping on the transition-metal lattice site, leading to a spin-state transition and influencing

DOI: 10.1021/jacs.6b08748
J. Am. Chem. Soc. 2016, 138, 14810−14819

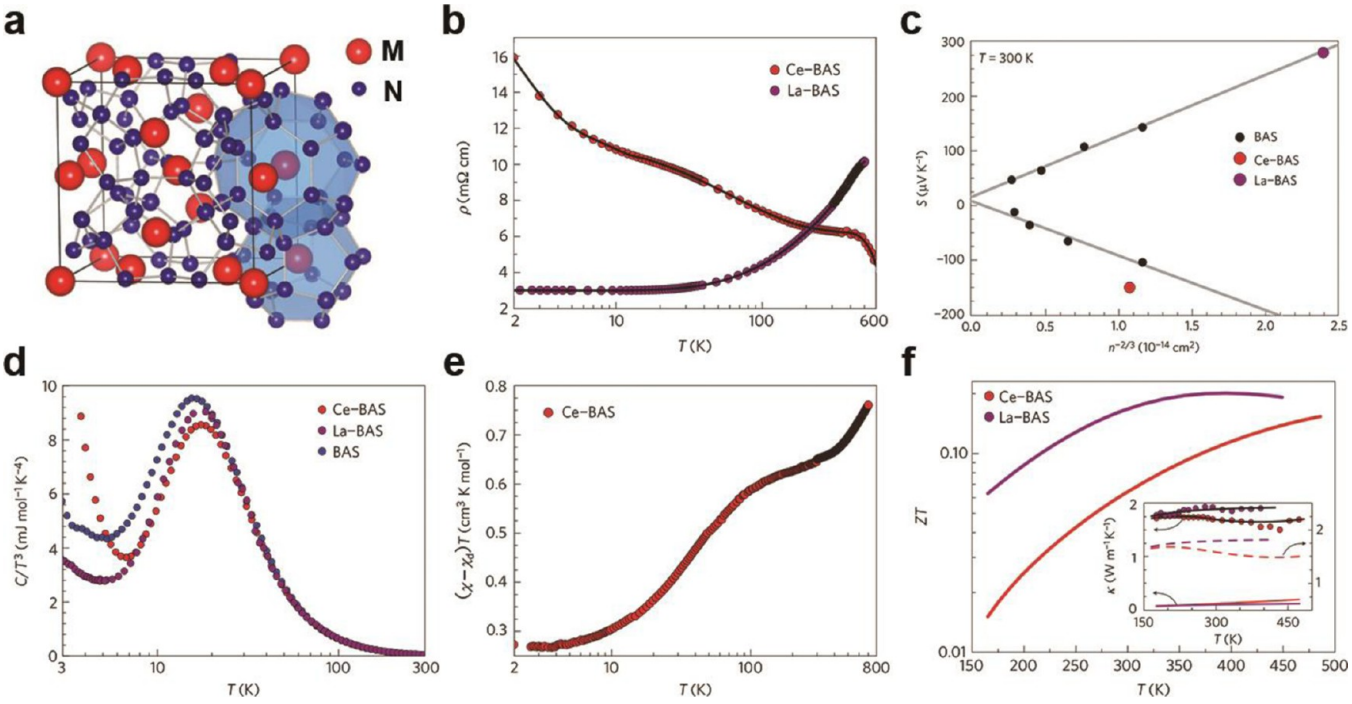

Figure 3. (a) Crystal structure model for type-I clathrates. The red guest atoms M are located in the cages constituted by the blue host atoms N. Note that M atoms occupy two different lattice sites (2a and 6d), which make up the cubic and tetragonal point symmetry. (b) Comparison of the temperature-dependent electrical resistivity for Ce-BAS and La-BAS. (c) Comparison of carrier density-dependent Seebeck coefficients for Ce-BAS and La-BAS. Data selected from published literature[58] for BAS samples with both carrier types and different concentrations are also shown for reference, with linear fitting. (d) Temperature-dependent specific heat curves plotted according to C/T^3 versus ln T for Ce-BAS, La-BAS, and BAS samples. (e) Temperature-dependent magnetic susceptibility curve plotted according to χT versus T for Ce-BAS, which reveals the paramagnetic contribution. (f) Temperature-dependent dimensionless figure of merit ZT for Ce-BAS and La-BAS. The inset shows the total thermal conductivity (symbols, left axis, κ) together with the electronic (solid lines, left axis, κ_e) and lattice parts (dashed lines, right axis, $\kappa_l = \kappa - \kappa_e$), estimated using the Wiedemann–Franz law. Adapted with permission from ref 40. Copyright 2013 Nature Publishing Group.

the thermoelectric performance.[41,42] These defect-related spin effects are very important for thermoelectric optimization; however, they have long been neglected.

Spin Entropy. According to thermodynamic analysis, the Seebeck coefficient is defined as the entropy density carried by a unit charge carrier as it moves,[38,47] which means that the more entropy it carries, the larger Seebeck coefficient it can possess. However, it is worth noting that, in addition to its charge degree of freedom, the electron's spin can also carry entropy flow, which indicates that spin entropy can be used as a new degree of freedom for modulating the Seebeck coefficient.[38,48−51] In most compounds, the spin contribution to the total entropy current can be ignored. However, it was reported to dominate the entropy current in materials with strong electron−electron interactions, as can be found in Co-based thermoelectric $Na_xCo_2O_4$[38,50] and $Ca_3Co_4O_9$,[51] and thus it can be used to tune the Seebeck coefficient. For example, in the Na_xCoO_2-based system, the spin entropy brought by Co ions endows it with a large Seebeck coefficient, which is higher by almost 1 order of magnitude compared to those of conventional metal and high-temperature superconductor thermoelectric systems. What's more, benefiting from the much enhanced Seebeck coefficient, the ZT performance at high temperatures reaches 0.8, which is a high value for oxide thermoelectrics and subverts the traditional cognition that oxide materials are not suitable for thermoelectric applications.

Inspired by the above concept, we also achieved the optimization of the Seebeck coefficient in I_2-II-IV-VI_4-type Cu_2ZnSnS_4 nanocrystal composites through using unpaired 3d electrons from the magnetic dopant as the new source of spin entropy.[39] More importantly, combined with narrowed band gap and enhanced bond anharmonicity caused by doping, the three necessary conditions for achieving high ZT—large electrical conductivity, high Seebeck coefficient, and low thermal conductivity—can be met simultaneously. Cu_2ZnSnS_4 is a wide band gap semiconductor adopting the distorted chalcopyrite-like structure, which endows it with a pretty low lattice thermal conductivity and promising high ZT performance. Benefiting from the above-mentioned advantages, we first synthesized pure and Ni-doped Cu_2ZnSnS_4 nanocrystals, and we performed electron paramagnetic resonance (EPR) experiments to study the effect of magnetic ion incorporation. As shown in Figure 2a,b, when Zn^{2+} was partly substituted by Ni^{2+}, in addition to the Zn nuclear spins (^{67}Zn, $I = 5/2$)-induced six-line hyperfine spectrum splitting and surface defects-induced single symmetric line located at $g = 1.996$, two additional lines that corresponded to $g = 2.23$ and 2.06 were also observed, which can be ascribed to the Ni^{2+} electron spin, indicating that Ni^{2+} doping brought more spin into Cu_2ZnSnS_4. More importantly, as the temperature increases, larger entropy flow can be gained from the Ni^{2+} electron spin, as evidenced by the enhanced EPR intensity when the temperature is raised from 300 to 590 K, which finally gave rise to a remarkably enhanced Seebeck coefficient. Subsequently, to verify the universality of spin entropy tuning by magnetic doping, fully substituted Cu_2XSnS_4 (X = Fe, Mn, Co) nanocrystals with different magnetic ions were synthesized and extensively investigated. The results have demonstrated that magnetic dopants with smaller electro-

DOI: 10.1021/jacs.6b08748
J. Am. Chem. Soc. 2016, 138, 14810−14819

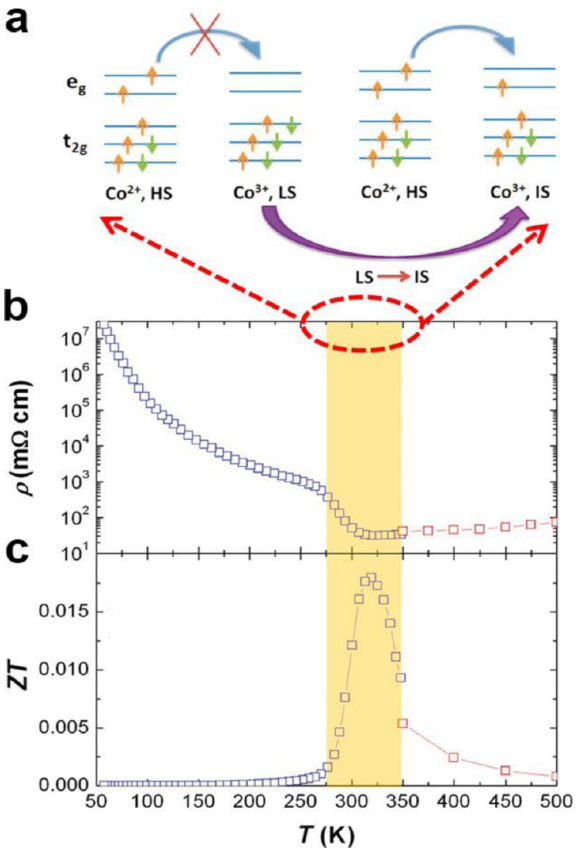

Figure 4. (a) Schematic illustration of the e_g electron hopping modes between Co^{2+} HS and Co^{3+} LS sates, as well as between Co^{2+} HS and Co^{3+} IS states. (b,c) Temperature dependence of resistivity (b) and dimensionless ZT (c) of $La_{0.94}Ce_{0.06}CoO_3$. The yellow area indicates the temperature range of the LS−IS transition, where notable changes in thermoelectric performance are seen. Adapted with permission from ref 41. Copyright 2010 American Chemical Society.

negativity but larger ionic radius differences from the constituent elements and larger crystal field stabilization energy are favorable for thermoelectric enhancement. Because of these improvements, the ZT value of Ni-doped Cu_2ZnSnS_4 nanocrystals is significantly improved by 7.4 times compared to that of the pristine counterpart, while a 9.2 times enhancement is found for the fully Co^{2+}-substituted Cu_2ZnSnS_4 nanocrystals (as seen in Figure 2c). Therefore, the above results have demonstrated that spin-entropy modulation can be seen as a new choice, derived from defect engineering, which may achieve the independent manipulation of the inversely coupled thermoelectric parameters.

Kondo Effect. According to the thermodynamic definition as stated above, we may expect that the Seebeck coefficient can be affected by charge carriers' interactions with the local magnetic moment in a magnetic solid (i.e., Kondo interaction/effect).[38,47] Recently, in strongly correlated compounds, especially those involving actinide elements like U and rare earth elements like Yb and Ce, high power factors (most of which have giant Seebeck coefficient values) have been discovered, which can be traced back to the Kondo interaction between conduction electrons and local unpaired 4f states.[52,53]

In a non-magnetic metallic system with magnetic impurities (like dilute magnetic alloys), the resistance show an unusual minimum as the temperature approaches 0 K,[54] and its origin puzzled the scientific community for a long time, until early in the 1960s, when Van den Berg recognized that[55] the resistance minimum was related to magnetic impurities in the non-magnetic host, which could induce local magnetic moments due to the spin of unpaired electrons in their atomic-like d or f shells. In 1964, Kondo[56] first calculated the problem using third-order perturbation theory and showed that the magnetic impurity and conducting electron exchanged their internal spin states, which contributed to a rise in the resistivity as the temperature approached 0 K and left a resistance minimum.[57]

It is worthy of note that the resulting electron scattering via magnetic impurities due to the Kondo effect can be seen as resonance scattering. This means that the scattering process has great energy asymmetry—i.e., the scattering intensity depends on the energy of electron—which can increase the Seebeck coefficient significantly. This kind of scattering mechanism usually occurs at low temperatures (below the Kondo temperature), while at room temperature and above, the phonon scattering process dominates, which is energy-independent. However, it was reported that, in some special cases (spin−phonon coupling etc.), the Kondo scattering scale can be extended to the high temperature range.[40] In a Ce-incorporated $Ba_8Au_xSi_{46-x}$ system (Ce-BAS), the 4f states associated with Ce guest ions induced a Kondo effect at low temperature (several K), leading to a resistivity contribution proportional to $-\ln T$ and significantly reduced carrier mobility. What's more, due to the spin-phonon interaction, the Kondo scattering scale was extended from ∼6 to the ∼120−400 K range and gave rise to an anomalous enhancement of S (Figure 3c), compared to those of pristine BAS[58] and its 4f-free counterpart, the La-incorporated $Ba_8Au_xSi_{46-x}$ system (La-BAS). According to the Anderson−Holstein model, in strong electron correlation system like BAS, the Kondo energy scale can be improved significantly, benefiting from the considerable electron−phonon interaction. Meanwhile, experiments have found that rattling is the characteristic phonon model in this system, as evidenced by the results that Ce substitution at the Ba sites in BAS gave rise to a notable enhancement of the atomic displacement parameter (i.e., rattling amplitude), while the Einstein-like contribution to the specific heat did not change much (as shown in Figure 3d). On the other hand, due to the thermally activating nature of the rattling process, these rattling-like local phonon modes in clathrates can be populated only at increased temperatures, which led to a substantial renormalization of the Kondo energy scale, as supported by the temperature-dependent magnetic susceptibility (Figure 3e).

The above results show that the Kondo-type interaction between Ce rattling modes in the cages and conductive electrons in the framework of $Ba_{6.91}Ce_{1.06}Au_{5.56}Si_{40.47}$ effectively extends the system's Kondo temperature and leads to a much enhanced Seebeck coefficient compared to the value of the pristine counterpart. These findings point out a new direction for using Kondo interactions to optimize the thermoelectric performance.

Spin-State Transition. As is known to all, rich spin states are widespread in transition-metal oxides like $LaCoO_3$ and $Ca_3Co_4O_9$, and they can be modified by stacking faults or aliovalent doping on the transition-metal lattice sites, leading to a spin-state transition,[42,59,60] which can be used to modulate the thermoelectric properties. For example, in Ce-doped $LaCoO_3$,[41] whose charge transport process is strongly governed by the spin states of the ground-state Co^{3+}, substitution of La^{3+} with Ce^{4+} brings Co^{2+} ions into Co^{3+} matrix. Co^{2+} always shows a high-spin state (HS, $t^2g^5e_g^2$), while Co^{3+} can show a low-spin state (LS, t^2g^6) or an intermediate-spin state (IS, $t^2g^5e_g^1$), as illustrated in

DOI: 10.1021/jacs.6b08748
J. Am. Chem. Soc. 2016, 138, 14810−14819

Figure 4a. At low temperature, Co^{3+} ions adopted LS states which blocked e_g electron transport, and when the temperature rose, a LS−IS transition occurred, which destroyed the spin blockade and induced electron hopping between the Co^{2+} HS and Co^{3+} IS states. Owing to the above favorable spin transition, the temperature-dependent resistivity showed a sudden decrease, accompanied by an insulator-to-metal phase transition, while the Seebeck coefficient and thermal conductivity remained almost unchanged. Consequently, a ZT maximum was observed, as seen in Figure 4c. The existence of such an exciting spin transition behavior in transition-metal oxides-based thermoelectric systems may lead to new approaches for the design and optimization of thermoelectric oxides driven by spin-state transition.

DEFECT-MEDIATED ATOM OR CHARGE MIGRATION EFFECT

Defects, especially vacancy-type defects, can usually act as media for atom migration or exchange, due to the lower formation energy of the intermediate states. This can lead to newly generated phases when it happens at the crystal interface/surface or to disordered structure when it occurs within the crystal lattice. In the meantime, vacancies are electrically charged and surrounded by oppositely charged carriers. Thus, they can also serve as carrier centers and assistant charge transport by mediating charge transfer. Discovery and application of these aspects in thermoelectric research can usually bring unexpected surprises.

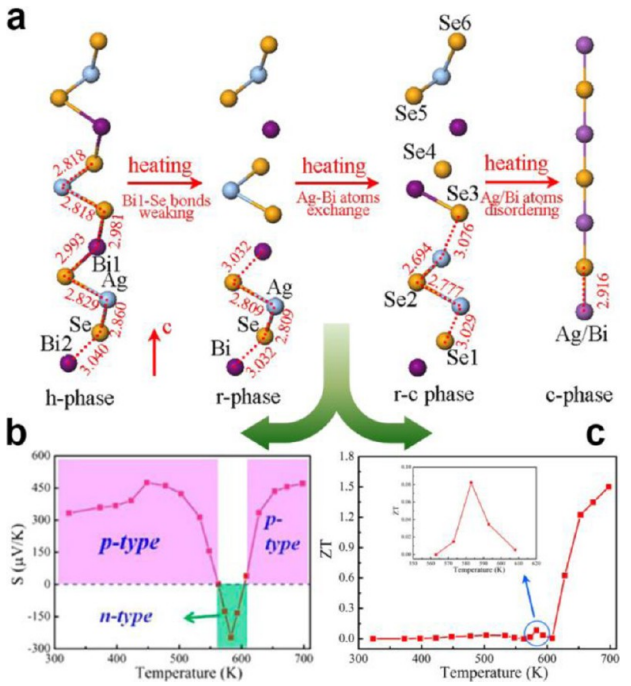

Figure 5. (a) Schematic illustration of the Ag vacancy-mediated Ag/Bi bimetal atom exchange in the Ag−Bi−Se chain during the rhombohedral-to-cubic phase transition, which leads to a reversible p-n-p switch. (b,c) Temperature-dependent Seebeck coefficient (b) and dimensionless ZT (c) for the $AgBiSe_2$ nanocrystal-based composite. The ZT value of $AgBiSe_2$ shows a maximum point during the phase transition and finally reaches 1.5 around 700 K, benefiting from the complete disordering of Ag/Bi atoms in the high-temperature phase. Adapted with permission from ref 43. Copyright 2012 American Chemical Society.

Defect-Mediated Atom Exchange. Defects, especially vacancy-type defects, can form intermediate low-energy states, which can serve as transfer stations for atom migration, resulting a newly generated phase or disordered structure,[61,62] both of which are favorable for thermoelectric modulation. For example, a recent study has found that, benefiting from a Ag vacancy-mediated Ag/Bi bimetal atom exchange, the thermoelectric properties of $AgBiSe_2$ can be adjusted accordingly.[43] As a p-type semiconductor originating from the intrinsic Ag vacancies, $AgBiSe_2$ undergoes a continuous phase transition from a room-temperature hexagonal phase to a medium-temperature rhombohedral phase, and then to high-temperature cubic phase. During this phase transition, Ag vacancy-mediated Ag/Bi bimetal atom exchange in the Ag−Bi−Se chain results in the newly generated Ag−Se−Ag chain with continuous electronic band distribution and an intermediate quasi-metallic state, which increases valence electron conduction and eventually leads to the reversible p-n-p switch, as shown in Figure 5. Meanwhile, a ZT maximum is observed around the phase transition temperature, just as found in the case of Ag_2X.[63] In addition, the complete disordering of Ag/Bi atoms in the high-temperature cubic phase gives impetus to the phonon−phonon umklapp scattering and causes much stronger bond anharmonicity, which significantly suppresses the lattice thermal conductivity. In the meantime, the high mobility of these disordering ions also contributes to a high electrical conductivity, which eventually leads to the highest ZT performance (ZT = 1.5 at 700 K). The discovery of this novel vacancy-mediated atom-exchange phenomenon with unusual thermoelectric performance presents us with another new choice for thermoelectric optimization.

Interlayer Charge Transfer. Vacancy, which breaks the continuity of chemical bonding by right of simultaneous atom and interatomic linkage deficiencies, has always been regarded as a class of very important phonon scattering sources for the reduction of thermal conductivity to promote the advancement of thermoelectric research. On the other hand, as is known, the vacancies are intrinsically constituted by a positively or negatively charged center surrounded by oppositely charged carriers. Thus, they can assistant charge transport by transfering charge carriers.[64−66] For example, recent experiments have shown that interlayer charge transfer can be achieved in BiCuSeO through the introduction of heterolayer Bi/Cu dual vacancies.[44] BiCuSeO possesses a unique layered structure consisting of alternating $[Bi_2O_2]^{2+}$ and $[Cu_2Se_2]^{2-}$ sublayers along the *c* axis, presenting us with a perfect platform for clear research on the effect of the dual vacancies. By means of co-instantaneous deficiencies of Bi and Cu atoms in the respective sublayers, Bi/Cu dual vacancies were successfully introduced into the system and induced a strong phonon scattering in the sample dominated by Bi/Cu dual vacancies, which brought about a maximum reduction of the thermal conductivity. More importantly, the interlayer charge transfer mediated by the existing Bi/Cu dual vacancies, as evidenced by positron annihilation spectrometry characterization, further enhanced the electrical conductivity while not changing the Seebeck coefficient (as seen in Figure 6). As consequence, the ZT value reached as high as 0.84 at the moderate temperature of 750 K in the Bi/Cu dual vacancies dominant sample (as shown in Figure 6e), which is superior to its counterparts in pristine as well as monovacancies samples. This vacancy-mediated charge-transfer effect, together with superior performance, undoubtedly demonstrates a novel avenue for rational research and optimization of high-performance thermoelectric materials.

DOI: 10.1021/jacs.6b08748
J. Am. Chem. Soc. 2016, 138, 14810−14819

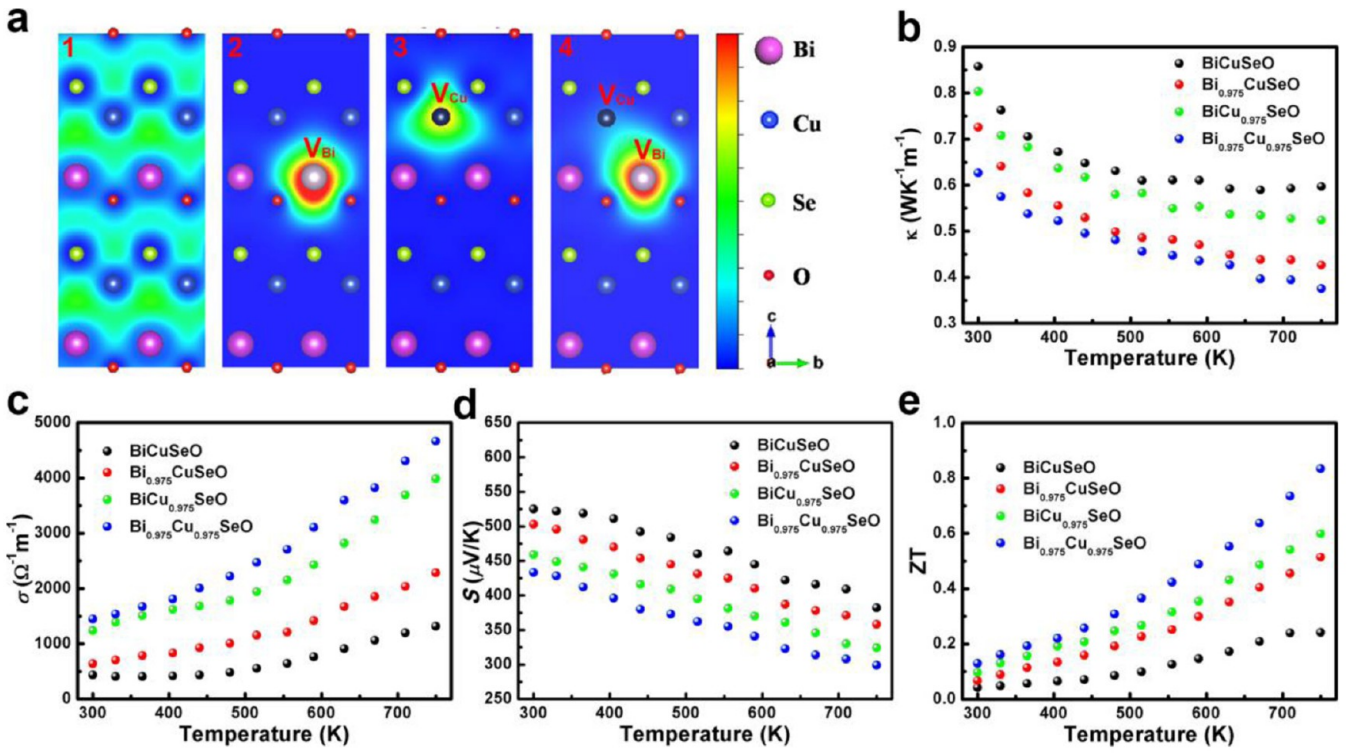

Figure 6. (a) Schematic graphs representing position and relative density of trapped positrons for $Bi_{1-x}Cu_{1-y}SeO$ samples in the (100) plane, based on positron annihilation spectrometry characterization and theoretical calculation. (b–e) Temperature dependences of the thermal conductivity (b), electrical conductivity (c), Seebeck coefficient (d), and dimensionless thermoelectric figure of merit (e) for $Bi_{1-x}Cu_{1-y}SeO$ samples. Adapted with permission from ref 44. Copyright 2015 American Chemical Society.

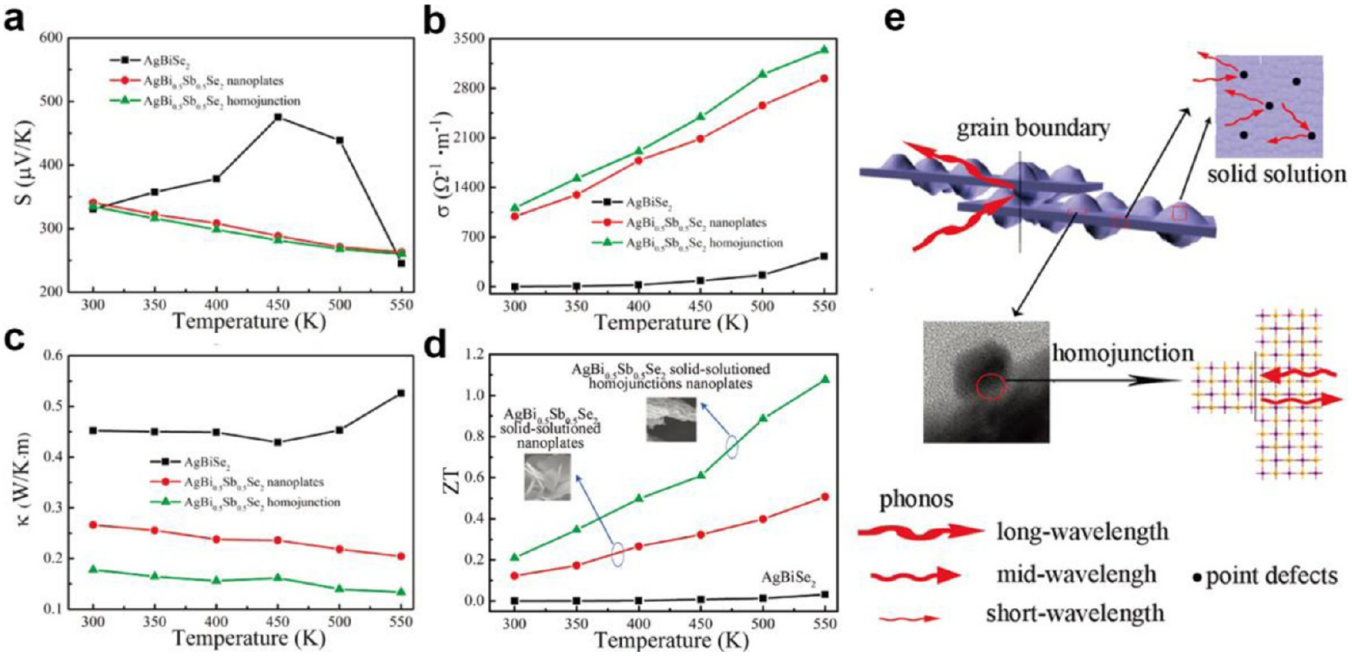

Figure 7. (a–d) Thermoelectric properties of $AgBiSe_2$-based samples. Temperature-dependent Seebeck coefficient (a), electrical conductivity (b), thermal conductivity (c), and dimensionless thermoelectric figure of merit (d) for $AgBiSe_2$ pristine nanoplates, $AgBi_{0.5}Sb_{0.5}Se_2$ solid-solution nanoplates, and $AgBi_{0.5}Sb_{0.5}Se_2$ solid-solutioned homojunction nanoplates. (e) Schematic illustration of the different phonon scattering models in $AgBi_{0.5}Sb_{0.5}Se_2$ solid-solution homojunctions. Adapted with permission from ref 45. Copyright 2012 American Chemical Society.

■ DEFECT-RELATED INTERFACE EFFECT

The nanostructuring approach has contributed to much of the recent achievements in pursuing high thermoelectric performance benefiting from the advantages of abundant interfaces resulting from planar-type defects, including grain/phase boundaries, stacking faults, hetero-/homojunctions, and distorted surfaces. Worthy of note is that interfaces can influence all three thermoelectric parameters; thus, the introduction of

DOI: 10.1021/jacs.6b08748
J. Am. Chem. Soc. 2016, 138, 14810–14819

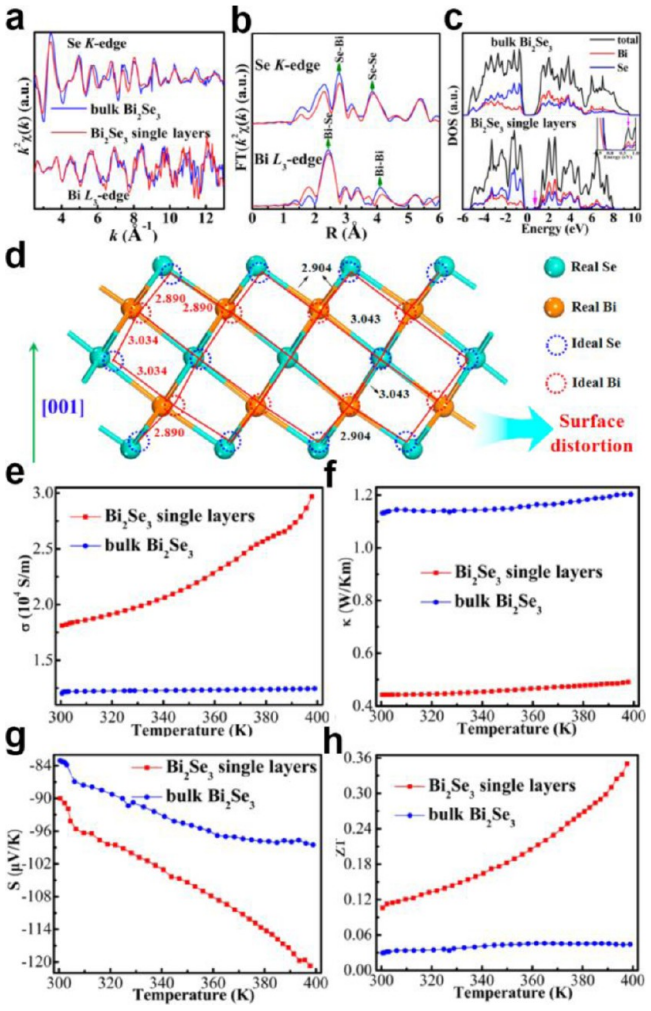

Figure 8. (a,b) $k^2\chi(k)$ oscillation curves of Bi L_3-edge and Se K-edge (a) from extended XAFS, and the corresponding Fourier transformation (b) for Bi_2Se_3 single layers (red line) and commercial bulk powder (blue line). (c) Calculated PDOS and DOS for single-layer and bulk Bi_2Se_3. Inset shows the enhanced DOS at the conduction band maximum for the single-layer Bi_2Se_3. (d) Two-dimensional structural model for Bi_2Se_3 single layer. (e–h) Temperature dependences of the electrical conductivity (e), thermal conductivity (f), Seebeck coefficient (g), and dimensionless ZT (h) for SLB composite and bulk Bi_2Se_3. Adapted with permission from ref 46. Copyright 2012 American Chemical Society.

interfaces into these nanostructured thermoelectrics can play an important role for tailoring their ZT performance.[67] On one hand, interfaces are beneficial for reduction of the thermal conductivity by blocking phonon propagation, and for enhancing the Seebeck coefficient in some special cases, like the interfacial filtering effect. However, at the same time, interfaces are also detrimental to the electrical transport process due to inevitable carrier scattering. Given that S is less influenced, improving ZT by the nanostructuring approach requires that reduction in the thermal conductivity should compensate and exceed the negative effect on the carrier mobility resulting from interface scattering.[68−70] Therefore, controllable manipulation of interfaces to balance their effects on electronic and thermal conductivities is critical for modifying the ZT performance in nanostructured thermoelectrics. In this regard, the homojunction strategy and surface distortion based on an ultrathin two-dimensional structure offer promising solutions.

Homojunction. In nanostructure-based thermoelectrics, introduction of heterostructures is accepted as an effective means to lower the thermal conductivity originating from interfacial phonon scattering, which has been extensively used in recent research.[71] But an unfortunate side effect of the use of heterosturctures is that, due to different compositions at the heterojunctions, they can scatter carriers at the same time, which is detrimental to high electrical conductivity. Unlike heterojunctions, homojunctions are built with the same composition, which seems to be favorable for minimum deterioration in electrical conductivity while also efficiently reducing the thermal conductivity. However, investigation on the effects of homojunctions has been long neglected in thermoelectric research.[45]

In our previous work, we put forward that the solid-solutioned homojunction concept can serve as an effective way to balance the effects of interfaces and synergistically optimize the thermoelectric parameters in a high-temperature disordered lattice.[45] For example, Sb-doped $AgBiSe_2$ solid-solutioned nanoplates with homojunctions were successfully synthesized for the first time and served as a platform for investigation of the effect of homojunctions. Experimental results elucidated that Sb doping can stabilize the non-ambient high-conductive phase to room temperature, which ensured that high electrical conductivity, only available at high temperatures before, can now be acquired over the whole temperature range (as seen in Figure 7b). What's more, the homojunctions generated in situ on the surface of $AgBi_{0.5}Sb_{0.5}Se_2$ nanoplates not only solved the dilemma of deterioration in electrical conductivity originating from interfacial scattering as occurred in heterojunctions, showing an unexpected increase, but also resulted in further reduction of the thermal conductivity by additional scattering of mid-wavelength phonons. As a result, the thermoelectric ZT of solid-solutioned $AgBi_{0.5}Sb_{0.5}Se_2$ was significantly increased from 0.03 (pristine $AgBiSe_2$, at 550 K) to 0.51, and further increased to 1.07 when homojunctions were added (as seen in Figure 7), benefiting from an unexpected increase in the electrical conductivity, together with a further reduction of thermal conductivity caused by homojunctions. These results indicate that the homojunction strategy can be a promising solution for balancing the effects of interfaces in nanostructure-based thermoelectrics and serve as new degree of freedom to synergistically modulate the intercoupled thermoelectric parameters.

Surface Distortion. As the surface of a crystal or crystallite, interfaces have particular atomic structures with the disruption of interatomic bonds, which endow them with a positive surface energy and make them intrinsically less energetically favorable than the bulk material. According to the principle of minimum energy, surface energy tends to minimize its value to maintain the thermodynamically stable state. Therefore, interfaces are very important in systems with big surface area-to-volume ratios, such as ultrathin two-dimensional nanosheets. Studies have shown that,[72−74] when a material is reduced to atomic thickness, the large specific surface energy (the ratio of surface energy per unit volume) makes the system very unstable. In this regard, surface distortions, like changes in interatomic distance and local atomic coordination, and distorted bond lengths and angles, are usually found at the interfaces, which can minimize the surface energy and stabilize the lattice structure. Obviously, these distorted interfaces would inevitably affect the electronic properties of the host, and they may serve as an independent degree of freedom to modify the potential thermoelectric performance.

DOI: 10.1021/jacs.6b08748
J. Am. Chem. Soc. 2016, 138, 14810−14819

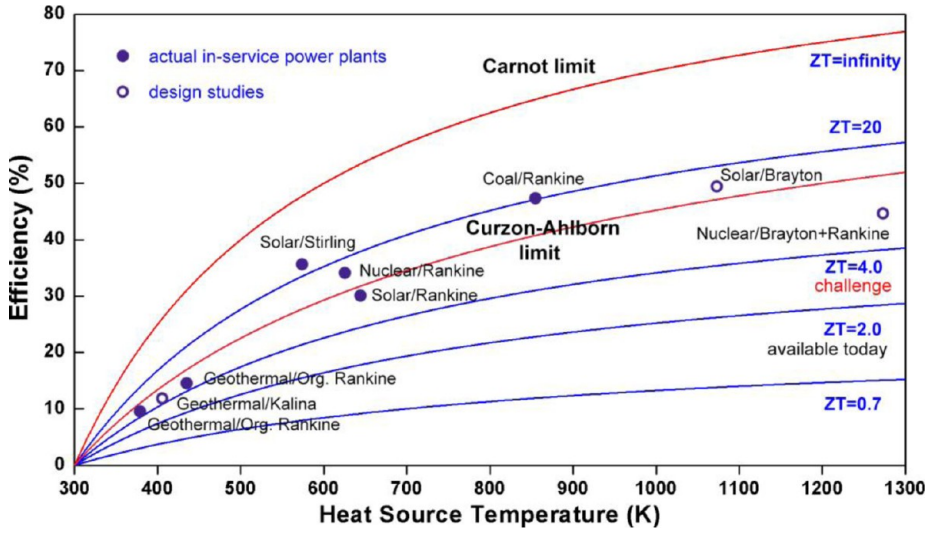

Figure 9. Efficiency of thermoelectric devices at different ZT values and T_{hot} (T_{cold} = 300 K, $\eta_{TE} = \frac{\sqrt{1+ZT}-1}{\sqrt{1+ZT}+T_{cold}/T_{hot}}\eta_C$). Efficiency of conventional mechanical engines together with the Carnot limit (ideal, reversible heat engine, $\eta_C = 1 - T_{cold}/T_{hot}$) and the Curzon–Ahlborn limit (endoreversible heat engine considering the irreversibility of heat transfer, $\eta_{CA} = 1 - \sqrt{T_{cold}/T_{hot}}$) is also shown. T_{cold} and T_{hot} are the absolute temperature of the cold and hot sides. Adapted from ref 10. Copyright 2009 Nature Publishing Group.

Taking Bi_2Se_3 as an example, Sun and co-workers[46] synthesized ultrathin Bi_2Se_3 nanosheets with atomic-level thickness, which were then fabricated into single-layer-based (SLB) nanocomposites to investigate their thermoelectric properties. Local atomic structure characterization by synchrotron-radiation X-ray absorption fine structure (srXAFS) spectra unambiguously elucidated that, in order to maintain its structural stability when the thickness reached atomic level, surface distortion occurred on the interface of the Bi_2Se_3 nanosheet, showing a much enhanced degree of lattice disorder together with slightly elongated interatomic distances compared to their bulk counterpart (Figure 8a–c). Moreover, first-principles calculations also revealed a much enhanced density of states (DOS) at the conduction band edge (Figure 8d), which is beneficial for electrical transport, as evidenced by the 2 times improvement in electrical conductivity of the SLB nanocomposite. Further research indicated that this surface distortion, in cooperation with the abundant interfaces, can enable selective scattering of the whole wavelength phonons rather than electrons, thus contributing to a reduction in thermal conductivities with no deterioration in electrical conductivity. In addition, the strong two-dimensional electron gas and "interface carrier filtering" effect also helped to improve the Seebeck coefficient, which finally resulted in a relative high ZT value (ZT = 0.35 at 400 K) for the SLB nanocomposite, about 8 times enhancement when compared to its bulk counterpart (as shown in Figure 8h). This newly discovered surface distortion effect demonstrates the superiority of interface structural disorder for synergistic modulation of the inverse-coupled thermoelectric parameters in nanostructured composites, when used in cooperation with other optimization strategies like interface energy filtering.

■ CONCLUSIONS AND PERSPECTIVES

Defect engineering leads to substantial improvement of the ZT performance that makes the field of thermoelectric study fertile for future waste heat recovery and solid refrigeration technological applications with precisely tailored properties. The present Perspective conveys the flavor of the defect engineering culture and emphasizes the pervasive role of defects in modulating the parameters that govern the ZT performance. However, divested of the mature established strategies for optimization of electronic and phonon structures based on defect engineering, we focus our interests, in this Perspective, on the under-exploited aspects of defect engineering, which include defect-related spin effects, defect-mediated atom or charge migration effects, and defect-related interface effects. As described above, the spin behavior of a thermoelectric solid can be tuned by crystal defects, leading to spin-entropy changes, Kondo interactions, and/or spin-state transitions, which would modify the thermoelectric parameters. In addition, vacancy-type defects can usually act as media for atom migration or charge exchange, which lead to a newly generated phase or disordered structure, and mediate charge transfer. Design and application of these aspects in thermoelectric research usually bring unexpected surprises. In the end, controllable manipulation of interfaces to balance their effects on electronic and thermal conductivities is critical for modifying the ZT performance. The homojunction strategy and surface distortion induced by introduction of defects provide promising solutions by maintaining the high electronic conductivity while effectively reducing κ_l. Through these new perspectives, we hope to combine the long-neglected parts of defect engineering with the current optimization strategies from the perspective of multiple degrees of freedom modulation, and we expect this to enable defect engineering to perform at full potential for boosting thermoelectric performance.

Reviewing the history of thermoelectric technology, a boom in academic research and breakthroughs of ZT values are always promoted by new concepts and ideas. From the semiconductor and alloy concept proposed by Ioffe in the early 1950s to the nanostructure approach established by Hicks and Dresselhaus, together with the PGEC concept put forward by Slack in the late 1990s, ZT has penetrated the threshold of 1 and 2 successively, reaching a state-of-the-art value of 2.6 recently.[75] On the other hand, when it comes to practical applications for direct heat-to-electricity conversion, thermoelectric devices are unlikely to

DOI: 10.1021/jacs.6b08748
J. Am. Chem. Soc. 2016, 138, 14810–14819

replace conventional mechanical engines in the near future.[10,76] When competing with existing mechanical heat engines, ZT values greater than 3.0 are needed; a device with a ZT value higher than 4 may have the potential to dominate the market (as seen in Figure 9).[6,10] Therefore, there is still a long way to go to achieve the large-scale commercial application of thermoelectric technology. We expect that the idea of multiple degrees of freedom modulation will lead researchers to some new thoughts and stimulate a new round of prosperity in thermoelectric studies.

For future research in this field, we think that a controlled study of the defects in thermoelectric solids is of critical importance. This means that intentional control of the type, size, concentration, and spatial distribution of defects is needed. Also, new methods and tools must be developed to precisely introduce and characterize defects in the lattice, together with new theoretical simulation method to model the structure−property relationship. There is no doubt that following such an integral approach will help in accelerating progress for thermoelectric applications. In conclusion, defect engineering is definitely at the core of thermoelectric research, and we are confident that, with the multiple degrees of freedom modulation idea in mind, breakthroughs in thermoelectric technology will certainly be unraveled in the decades to come.

AUTHOR INFORMATION

Corresponding Authors

*cxiao@ustc.edu.cn

*yxie@ustc.edu.cn

Notes

The authors declare no competing financial interest.

ACKNOWLEDGMENTS

This work was financially supported by National Basic Research Program of China (2015CB932302), National Natural Science Foundation of China (21622107, 21401182, 21331005, 11321503, 91422303, and U1532265), the Youth Innovation Promotion Association CAS (2016392), the Key Laboratory of Neutron Physics (CAEP 2014DB02), and the Fundamental Research Funds for the Central University (WK2340000075, WK2340000063, and WK2060190027).

REFERENCES

(1) Wise, M.; Calvin, K.; Thomson, A.; Clarke, L.; Bond-Lamberty, B.; Sands, R.; Smith, S. J.; Janetos, A.; Edmonds, J. *Science* **2009**, *324*, 1183.

(2) Chu, S.; Majumdar, A. *Nature* **2012**, *488*, 294.

(3) Dresselhaus, M. S.; Thomas, I. L. *Nature* **2001**, *414*, 332.

(4) Armstrong, R. C.; Wolfram, C.; de Jong, K. P.; Gross, R.; Lewis, N. S.; Boardman, B.; Ragauskas, A. J.; Ehrhardt-Martinez, K.; Crabtree, G.; Ramana, M. V. *Nat. Energy* **2016**, *1*, 15020.

(5) Zeier, W. G.; Schmitt, J.; Hautier, G.; Aydemir, U.; Gibbs, Z. M.; Felser, C.; Snyder, G. J. *Nat. Rev. Mater.* **2016**, *1*, 16032.

(6) Bell, L. E. *Science* **2008**, *321*, 1457.

(7) Kim, S. I.; Lee, K. H.; Mun, H. A.; Kim, H. S.; Hwang, S. W.; Roh, J. W.; Yang, D. J.; Shin, W. H.; Li, X. S.; Lee, Y. H.; Snyder, G. J.; Kim, S. W. *Science* **2015**, *348*, 109.

(8) Zhao, L. D.; Tan, G.; Hao, S.; He, J.; Pei, Y.; Chi, H.; Wang, H.; Gong, S.; Xu, H.; Dravid, V. P.; Uher, C.; Snyder, G. J.; Wolverton, C.; Kanatzidis, M. G. *Science* **2016**, *351*, 141.

(9) Shi, X.; Chen, L. *Nat. Mater.* **2016**, *15*, 691.

(10) Vining, C. B. *Nat. Mater.* **2009**, *8*, 83.

(11) Xiao, C.; Li, Z.; Li, K.; Huang, P. C.; Xie, Y. *Acc. Chem. Res.* **2014**, *47*, 1287.

(12) Urban, J. J. *Nat. Nanotechnol.* **2015**, *10*, 997.

(13) Goldsmid, H. J. In *CRC Handbook of Thermoelectrics*; Rowe, D. M., Ed.; CRC Press: Boca Raton, FL, 1995; p 74.

(14) Sootsman, J. R.; Chung, D. Y.; Kanatzidis, M. G. *Angew. Chem., Int. Ed.* **2009**, *48*, 8616.

(15) Beekman, M.; Morelli, D. T.; Nolas, G. S. *Nat. Mater.* **2015**, *14*, 1182.

(16) Liu, Y.; Zhou, M.; He, J. *Scr. Mater.* **2016**, *111*, 39.

(17) Kimerling, L. C. *MRS Bull.* **1991**, *16*, 42.

(18) Tuller, H. L.; Bishop, S. R. *Annu. Rev. Mater. Res.* **2011**, *41*, 369.

(19) Wang, H.; Zhang, J.; Hang, X.; Zhang, X.; Xie, J.; Pan, B.; Xie, Y. *Angew. Chem.* **2015**, *127*, 1211.

(20) Hu, L.; Zhu, T.; Liu, X.; Zhao, X. *Adv. Funct. Mater.* **2014**, *24*, 5211.

(21) Jiang, G.; He, J.; Zhu, T.; Fu, C.; Liu, X.; Hu, L.; Zhao, X. *Adv. Funct. Mater.* **2014**, *24*, 3776.

(22) Zhu, T.; Hu, L.; Zhao, X.; He, J. *Adv. Sci.* **2016**, *3*, 1600004.

(23) Park, J. G.; Lee, Y. H. *Curr. Appl. Phys.* **2016**, *16*, 1202.

(24) Lan, J. L.; Liu, Y.; Lin, Y. H.; Nan, C. W.; Cai, Q.; Yang, X. *Sci. Rep.* **2015**, *5*, 7783.

(25) Balandin, A. A.; Nika, D. L. *Mater. Today* **2012**, *15*, 266.

(26) Peng, K.; Lu, X.; Zhan, H.; Hui, S.; Tang, X.; Wang, G.; Dai, J.; Uher, C.; Wang, G.; Zhou, X. *Energy Environ. Sci.* **2016**, *9*, 454.

(27) Wei, T. R.; Tan, G.; Zhang, X.; Wu, C. F.; Li, J. F.; Dravid, V. P.; Snyder, G. J.; Kanatzidis, M. G. *J. Am. Chem. Soc.* **2016**, *138*, 8875.

(28) Zhang, Q.; Liao, B.; Lan, Y.; Lukas, K.; Liu, W.; Esfarjani, K.; Opeil, C.; Broido, D.; Chen, G.; Ren, Z. *Proc. Natl. Acad. Sci. U. S. A.* **2013**, *110*, 13261.

(29) Tan, G.; Zhao, L. D.; Shi, F.; Doak, J. W.; Lo, S. H.; Sun, H.; Wolverton, C.; Dravid, V. P.; Uher, C.; Kanatzidis, M. G. *J. Am. Chem. Soc.* **2014**, *136*, 7006.

(30) Tan, G.; Shi, F.; Hao, S.; Chi, H.; Zhao, L. D.; Uher, C.; Wolverton, C.; Dravid, V. P.; Kanatzidis, M. G. *J. Am. Chem. Soc.* **2015**, *137*, 5100.

(31) Zhao, L. D.; Zhang, X.; Wu, H.; Tan, G.; Pei, Y.; Xiao, Y.; Chang, C.; Wu, D.; Chi, H.; Zheng, L.; Gong, S.; Uher, C.; He, J.; Kanatzidis, M. G. *J. Am. Chem. Soc.* **2016**, *138*, 2366.

(32) Heremans, J. P.; Jovovic, V.; Toberer, E. S.; Saramat, A.; Kurosaki, K.; Charoenphakdee, A.; Yamanaka, S.; Snyder, G. J. *Science* **2008**, *321*, 554.

(33) Biswas, K.; He, J. Q.; Blum, I. D.; Wu, C. I.; Hogan, T. P.; Seidman, D. N.; Dravid, V. P.; Kanatzidis, M. G. *Nature* **2012**, *489*, 414.

(34) Pei, Y.; Shi, X.; LaLonde, A.; Wang, H.; Chen, L.; Snyder, G. J. *Nature* **2011**, *473*, 66.

(35) Pei, Y. L.; Wu, H.; Wu, D.; Zheng, F.; He, J. *J. Am. Chem. Soc.* **2014**, *136*, 13902.

(36) Duan, B.; Yang, J.; Salvador, J. R.; He, Y.; Zhao, B.; Wang, S.; Wei, P.; Ohuchi, F. S.; Zhang, W.; Hermann, R. P.; Gourdon, O.; Mao, S. X.; Cheng, Y.; Wang, C.; Liu, J.; Zhai, P.; Tang, X.; Zhang, Q.; Yang, J. *Energy Environ. Sci.* **2016**, *9*, 2090.

(37) Fu, C.; Bai, S.; Liu, Y.; Tang, Y.; Chen, L.; Zhao, X.; Zhu, T. *Nat. Commun.* **2015**, *6*, 8144.

(38) Wang, Y.; Rogado, N. S.; Cava, R. J.; Ong, N. P. *Nature* **2003**, *423*, 425.

(39) Xiao, C.; Li, K.; Zhang, J. J.; Tong, W.; Liu, Y. W.; Li, Z.; Huang, P. C.; Pan, B. C.; Su, H. B.; Xie, Y. *Mater. Horiz.* **2014**, *1*, 81.

(40) Prokofiev, A.; Sidorenko, A.; Hradil, K.; Ikeda, M.; Svagera, R.; Waas, M.; Winkler, H.; Neumaier, K.; Paschen, S. *Nat. Mater.* **2013**, *12*, 1096.

(41) Wang, Y.; Sui, Y.; Wang, X. J.; Su, W. H.; Cao, W. W.; Liu, X. Y. *ACS Appl. Mater. Interfaces* **2010**, *2*, 2213.

(42) Klie, R. F.; Qiao, Q.; Paulauskas, T.; Gulec, A.; Rebola, A.; Öğüt, S.; Prange, M. P.; Idrobo, J. C.; Pantelides, S. T.; Kolesnik, S.; Dabrowski, B.; Ozdemir, M.; Boyraz, C.; Mazumdar, D.; Gupta, A. *Phys. Rev. Lett.* **2012**, *108*, 196601.

(43) Xiao, C.; Qin, X. M.; Zhang, J.; An, R.; Xu, J.; Li, K.; Cao, B. X.; Yang, J. L.; Ye, B. J.; Xie, Y. *J. Am. Chem. Soc.* **2012**, *134*, 18460.

(44) Li, Z.; Xiao, C.; Fan, S.; Deng, Y.; Zhang, W.; Ye, B.; Xie, Y. *J. Am. Chem. Soc.* **2015**, *137*, 6587.

DOI: 10.1021/jacs.6b08748
J. Am. Chem. Soc. 2016, 138, 14810−14819

(45) Xiao, C.; Xu, J.; Cao, B. X.; Li, K.; Kong, M. G.; Xie, Y. *J. Am. Chem. Soc.* **2012**, *134*, 7971.
(46) Sun, Y. F.; Cheng, H.; Gao, S.; Liu, Q. H.; Sun, Z. H.; Xiao, C.; Wu, C. Z.; Wei, S. Q.; Xie, Y. *J. Am. Chem. Soc.* **2012**, *134*, 20294.
(47) Emin, D. In *Thermoelectrics Handbook: Macro to Nano*; Rowe, D. M., Ed.; CRC Press: Boca Raton, FL, 2006; p 5-2.
(48) Takeuchi, T.; Kondo, T.; Takami, T.; Takahashi, H.; Ikuta, H.; Mizutani, U.; Soda, K.; Funahashi, R.; Shikano, M.; Mikami, M.; Tsuda, S.; Yokoya, T.; Shin, S.; Muro, T. *Phys. Rev. B: Condens. Matter Mater. Phys.* **2004**, *69*, 125410.
(49) Koshibae, W.; Maekawa, S. *Phys. Rev. Lett.* **2001**, *87*, 236603.
(50) Wissgott, P.; Toschi, A.; Sangiovanni, G.; Held, K. *Phys. Rev. B: Condens. Matter Mater. Phys.* **2011**, *84*, 085129.
(51) Limelette, P.; Hardy, V.; Auban-Senzier, P.; Jérome, D.; Flahaut, D.; Hébert, S.; Frésard, R.; Simon, Ch.; Noudem, J.; Maignan, A. *Phys. Rev. B: Condens. Matter Mater. Phys.* **2005**, *71*, 233108.
(52) Jie, Q.; Hu, R.; Bozin, E.; Llobet, A.; Zaliznyak, I.; Petrovic, C.; Li, Q. *Phys. Rev. B: Condens. Matter Mater. Phys.* **2012**, *86*, 115121.
(53) Zlatić, V.; Monnier, R. P. *Phys. Rev. B: Condens. Matter Mater. Phys.* **2005**, *71*, 165109.
(54) De Haas, W. J.; De Boer, J.; Van dën Berg, G. J. *Physica* **1934**, *1*, 1115.
(55) Van den Berg, G. J. In *Progress in Low Temperature Physics*, Vol. *IV*; Gorter, C. J., Ed.; North-Holland Publishing Co.: Amsterdam, 1964; p 194.
(56) Kondo, J. *Prog. Theor. Phys.* **1964**, *32*, 37.
(57) Hewson, A. C.; Kondo, J. *Scholarpedia* **2009**, *4*, 7529.
(58) Aydemir, U.; Candolfi, C.; Ormeci, A.; Oztan, Y.; Baitinger, M.; Oeschler, N.; Steglich, F.; Grin, Y. *Phys. Rev. B: Condens. Matter Mater. Phys.* **2011**, *84*, 195137.
(59) Huang, Y.; Zhao, B.; Ang, R.; Lin, S.; Huang, Z.; Tan, S.; Liu, Y.; Song, W.; Sun, Y. *J. Phys. Chem. C* **2013**, *117*, 11459.
(60) Nekrasov, I. A.; Streltsov, S. V.; Korotin, M. A.; Anisimov, V. I. *Phys. Rev. B: Condens. Matter Mater. Phys.* **2003**, *68*, 235113.
(61) Casavola, M.; van Huis, M. A.; Bals, S.; Lambert, K.; Hens, Z.; Vanmaekelbergh, D. *Chem. Mater.* **2012**, *24*, 294.
(62) Shaughnessy, M. C.; Bartelt, N. C.; Zimmerman, J. A.; Sugar, J. D. *J. Appl. Phys.* **2014**, *115*, 063705.
(63) Xiao, C.; Xu, J.; Li, K.; Feng, J.; Yang, J. L.; Xie, Y. *J. Am. Chem. Soc.* **2012**, *134*, 4287.
(64) Chacon, G.; Long, X.; Zheng, C. *J. Alloys Compd.* **1995**, *216*, 177.
(65) Lyu, M.; Liu, Y.; Zhi, Y.; Xiao, C.; Gu, B.; Hua, X.; Fan, S.; Lin, Y.; Bai, W.; Tong, W.; Zou, Y.; Pan, B.; Ye, B.; Xie, Y. *J. Am. Chem. Soc.* **2015**, *137*, 15043.
(66) Xu, W.; Liu, Y.; Zhao, L. D.; An, P.; Lin, Y. H.; Marcelli, A.; Wu, Z. *J. Mater. Chem. A* **2013**, *1*, 12154.
(67) Medlin, D. L.; Snyder, G. J. *Curr. Opin. Colloid Interface Sci.* **2009**, *14*, 226.
(68) Sharp, J. W.; Poon, S. J.; Goldsmid, H. J. *Phys. Status Solidi A* **2001**, *187*, 507.
(69) Son, J. S.; Zhang, H.; Jang, J.; Poudel, B.; Waring, A.; Nally, L.; Talapin, D. V. *Angew. Chem., Int. Ed.* **2014**, *53*, 7466.
(70) Puneet, P.; Podila, R.; Zhu, S.; Skove, M. J.; Tritt, T. M.; He, J.; Rao, A. M. *Adv. Mater.* **2013**, *25*, 1033.
(71) Poudeu, P. F. P.; D'Angelo, J.; Kong, H.; Downey, A.; Short, J. L.; Pcionek, R.; Hogan, T. P.; Uher, C.; Kanatzidis, M. G. *J. Am. Chem. Soc.* **2006**, *128*, 14347.
(72) Sun, Y.; Sun, Z.; Gao, S.; Cheng, H.; Liu, Q.; Piao, J.; Yao, T.; Wu, C.; Hu, S.; Wei, S.; Xie, Y. *Nat. Commun.* **2012**, *3*, 1057.
(73) Sun, Y.; Liu, Q.; Gao, S.; Cheng, H.; Lei, F.; Sun, Z.; Jiang, Y.; Su, H.; Wei, S.; Xie, Y. *Nat. Commun.* **2013**, *4*, 2899.
(74) Liang, L.; Cheng, H.; Lei, F.; Han, J.; Gao, S.; Wang, C.; Sun, Y.; Qamar, S.; Wei, S.; Xie, Y. *Angew. Chem., Int. Ed.* **2015**, *54*, 12004.
(75) Zhao, L. D.; Lo, S. H.; Zhang, Y.; Sun, H.; Tan, G.; Uher, C.; Wolverton, C.; Dravid, V. P.; Kanatzidis, M. G. *Nature* **2014**, *508*, 373.
(76) Shakouri, A. *Annu. Rev. Mater. Res.* **2011**, *41*, 399.

DOI: 10.1021/jacs.6b08748
J. Am. Chem. Soc. 2016, 138, 14810−14819